PHYSICAL REVIEW B VOLUME 25, NUMBER 6 15 MARCH 1982

Theory of fine-structure splittings for donor-bound excitons in indirect materials

Yia-Chung Chang* and T. C. McGill
California Institute of Technology, Pasadena, California 91125
(Received 25 June 1981)

We present a theory for the fine structures in the electronic excitation spectra for excitons bound to various donors in Si and Ge. These fine structures are produced by the mixing of Hartree-Fock solutions through the interparticle interactions. We have calculated the excitation energies for the low-lying electronic excited states in the Hartree-Fock approximation, and estimated the fine-structure splittings using the first-order degenerate perturbation theory. The energy separations between these states and the ground state are in good agreement with the experimental data. The fine-structure terms are found to be small relative to the separation between states from different configurations for most donors in Si and Ge, thus allowing an interpretation of the spectra in terms of a shell model.

I. INTRODUCTION

Recently, there has been a considerable amount of interest in the excitation spectrum of the bound exciton (BE) and bound multiexciton complexes (BMEC). The luminescence due to the radiative recombination of excitons bound to neutral impurities in Si was first observed by Haynes[1] and later studied more extensively by Dean *et al.*[2] Kaminskii *et al.*[3] observed a series of sharp lines (known as the KAPS lines) in the luminescence spectra of lightly doped Si, which they attributed to the electron-hole recombination in the BMEC. The explanation of the origin of the KAPS lines was further strengthened by Sauer,[4] Kosai and Gershenzon,[5] and Dean *et al.*[6] Kirczenow[7] proposed a shell model for BE and BMEC, which appears to account for the major features of the experimental data.[8] This model has recently been reviewed in detail by Thewalt.[9]

In the shell model, many states of the same configuration are assumed to be degenerate; for example, the $\{2\Gamma_3;\Gamma_8\}$ (Refs. 7 and 9) state is 16-fold degenerate. In practice, the linear combinations of these states, which transform according to different representations of the tetrahedral group for the total Hamiltonian, are in general associated with different energy eigenvalues. For instance, the product states of two Γ_3 electrons can be decomposed into states transforming according to the Γ_1, Γ_2, and Γ_3 representations. The products of these states with the Γ_8 hole state can be further decomposed into states transforming according to the representations Γ_8, Γ_8, and $\Gamma_6+\Gamma_7+\Gamma_8$, respectively. Without including the interparticle interaction, it is not possible to predict these fine-structure splittings. Some of these fine-structure splittings have recently been observed for BE in Ge:P and Ge:As by Mayer and Lightowlers.[10] These lines cannot be explicitly identified without going beyond the shell model.

In the present paper, we present a theoretical calculation of the excitation spectrum for the donor bound exciton system (D^0X) in which interparticle interactions are properly taken into account. Fine-structure splittings for states of various configurations are obtained for several donors in Si and Ge. We find that the charge density of the electrons in the D^0X is ellipsoidally distributed. When the major axes of the ellipsoids associated with the two electrons are not oriented parallel to each other (e.g., two electrons localized in valleys on different axes) the mutual interaction between them (the nonparallel mutual interaction) is a few percent less than that for the case where the two major axes are parallel to each other (the parallel mutual interaction). This difference in parallel and nonparallel mutual interactions is the major source for the coupling between states of different configurations but of the same overall symmetry to which the two-electron product states belong, for example, the coupling between $(\Gamma_1\Gamma_1)\Gamma_1$, $(\Gamma_3\Gamma_3)\Gamma_1$, and $(\Gamma_5\Gamma_5)\Gamma_1$ states [where the notation $(\Gamma_3\Gamma_3)\Gamma_1$ means that two electrons of Γ_3 symmetry couple together to form a product state of Γ_1 symmetry].[11] The strength of this coupling depends

sensitively on the relative magnitude of the difference in parallel and nonparallel mutual interaction to the energy spacing between the states of various configurations. For example, the coupling for the ground state of configuration $(\Gamma_1\Gamma_1)\Gamma_1$ with states of other configurations but with Γ_1 total symmetry in Si:P is negligibly small (less than 0.1%), because this level is well separated in energy from the states it couples to. For some of the excited states, this coupling is substantial [e.g., the mixing between $(\Gamma_3\Gamma_3)\Gamma_1$ and $(\Gamma_5\Gamma_5)\Gamma_1$ state is about 10%].

In general, the hole wave function can be described by a spherical (*s*-like) wave function plus some admixture of a quadrupole (*d*-like) wave function. The electron-hole interaction, which mixes the *s*- and *d*-like components of the hole state, produces the coupling between states of different configurations but the same overall symmetry to which the total wave function belongs, for example, the coupling between $[(\Gamma_1\Gamma_5)\Gamma_5,\Gamma_8]\Gamma_8$ and $[(\Gamma_1\Gamma_1)\Gamma_1,\Gamma_8]\Gamma_8$ states (where the notation $[(\Gamma_1\Gamma_5)\Gamma_5,\Gamma_8]\Gamma_8$ means that a Γ_1 electron and a Γ_5 electron first couple together to form a product state of Γ_5 symmetry, which then couples to the Γ_8 hole state to form a new product state of Γ_8 symmetry). We find that the fine-structure splitting due to the electron-hole interaction is about 5 times smaller than the corresponding splitting in the free-exciton system. Our results for the energy spacings between various states are in good agreement with the experimental data available. A preliminary report on this work was presented in Ref. 12.

This paper is organized in the following way. In Sec. II, the general theory for solving the donor bound exciton is presented. In Sec. III, the calculation method is discussed. In Sec. IV, the results are discussed and the comparison with the experimental data is made. Finally, in Sec. V, we present our conclusion.

II. GENERAL THEORY

The D^0X is formed by attracting one hole to a D^- core.[11] Therefore the total Hamiltonian is equal to the sum of the Hamiltonian for a D^- system H_{D^-}, the single-particle Hamiltonian for a hole h_h, interacting with the donor and the electron-hole interaction terms. Namely,

$$H_{D^0X}=H_{D^-}(1,2)+h_h(3)-v(1,3)-v(2,3)\ , \tag{1}$$

where we have labeled the coordinates of the two core electrons by 1,2, and those of the hole by 3; the electron-hole interactions $v(1,3)$ and $v(2,3)$ have the same Fourier transform $v(\vec{q})$,

$$v(\vec{q})=\frac{4\pi e^2}{\epsilon(\vec{q})q^2}\ , \tag{2}$$

where $\epsilon(\vec{q})$ is the $\vec{q}$-dependent dielectric function.[13–15] We expand the exact eigenstate of H_{D^0X} in terms of products of two pseudo-Bloch-functions associated with the conduction band, $\phi^c_{\vec{k}_1}$ and $\phi^c_{\vec{k}_2}$, and one pseudo-Bloch-function associated with the valence band, $\phi^v_{\vec{k}_3}$, as

$$\Psi(\vec{r}_1,\vec{r}_2,\vec{r}_3)=\sum_{\vec{k}_1\vec{k}_2,\vec{k}_3} B(\vec{k}_1,\vec{k}_2,\vec{k}_3)\phi^c_{\vec{k}_1}(\vec{r}_1)\phi^c_{\vec{k}_2}(\vec{r}_2)\phi^v_{\vec{k}_3}(\vec{r}_3)\ . \tag{3}$$

The coefficients $B(\vec{k}_1,\vec{k}_2,\vec{k}_3)$ must satisfy the Schrödinger equation

$$H_{D^0X}B(\vec{k}_1,\vec{k}_2,\vec{k}_3)=EB(\vec{k}_1,\vec{k}_2,\vec{k}_3)\ , \tag{4}$$

where H_{D^0X} is an integral operator in $\vec{k}$ space defined by

$$\begin{aligned}H_{D^0X}B(\vec{k}_1,\vec{k}_2,\vec{k}_3)=&H_{D^-}(12)B(\vec{k}_1,\vec{k}_2,\vec{k}_3)-E_v(\vec{k}_3)B(\vec{k}_1,\vec{k}_2,\vec{k}_3)+\sum_{\vec{k}'_3}\langle\vec{k}_3\,|\,V_\phi\,|\,\vec{k}'_3\rangle B(\vec{k}_1,\vec{k}_2,\vec{k}'_3)\\&-\sum_{\vec{k}'_1\vec{k}'_3}\langle\vec{k}_1\vec{k}_3\,|\,v\,|\,\vec{k}'_1\vec{k}'_3\rangle B(\vec{k}'_1,\vec{k}_2,\vec{k}'_3)-\sum_{\vec{k}'_2\vec{k}'_3}\langle\vec{k}_2\vec{k}_3\,|\,v\,|\,\vec{k}'_2\vec{k}'_3\rangle B(\vec{k}_1,\vec{k}'_2,\vec{k}'_3)\ ,\end{aligned} \tag{5}$$

where $H_{D^-}(1,2)$ is the corresponding integral operator for the D^- system defined in Ref. 11, $E_v(\vec{k}_3)$ is the dispersion relation for the valence band measured from the top of the valence band, and V_ϕ is the impurity

pseudopotential. Since the hole wave function is localized near the zone center, it is a good approximation to replace $\langle \vec{k}_3 | V_\phi | \vec{k}_3' \rangle$ by the point-charge potential $V_{pc}(\vec{k}_3 - \vec{k}_3')$ as defined in Ref. 16. Expanding the products of the periodic parts of the pseudo-Bloch functions $u_{\vec{k}_1'}(\vec{r}_1) u_{\vec{k}_1}^*(\vec{r}_1)$ and $u_{\vec{k}_3'}(\vec{r}_3) u_{\vec{k}_3}^*(\vec{r}_3)$ in Fourier series with coefficients $c(\vec{k}_1, \vec{k}_1'; \vec{G}_1)$ and $c(\vec{k}_3, \vec{k}_3'; \vec{G}_3)$, respectively, we can write the electron-hole interaction as

$$\langle \vec{k}_1 \vec{k}_3 | v | \vec{k}_1' \vec{k}_3' \rangle = \sum_{\vec{G}_1 \vec{G}_3} \tilde{v}(\vec{G}_1 + \vec{k}_1 - \vec{k}_1') c(\vec{k}_1, \vec{k}_1'; \vec{G}_1) c^*(\vec{k}_3', \vec{k}_3; \vec{G}_3) \delta(\vec{G}_1 + \vec{k}_1 - \vec{k}_1' - \vec{G}_3 - \vec{k}_3' + \vec{k}_3) , \quad (6)$$

where $\vec{G}_1, \vec{G}_3$ are reciprocal-lattice vectors and $\delta(\vec{k})$ is the Dirac delta function. This term has appreciable contribution only when $\vec{k}_3$ and $\vec{k}_3'$ are near the zone center; therefore, the momentum conservation can be satisfied only if $\vec{G}_1 = 0$ and $\vec{G}_3 = 0$. Hence, we can write approximately

$$\langle \vec{k}_1' \vec{k}_3' | v | \vec{k}_1 \vec{k}_3 \rangle = \tilde{v}(\vec{k}_1 - \vec{k}_1') \delta(\vec{k}_1 - \vec{k}_1' - \vec{k}_3' + \vec{k}_3) . \quad (7)$$

Similarly, for the mutual interaction between the second electron and the hole,

$$\langle \vec{k}_2' \vec{k}_3' | v | \vec{k}_2 \vec{k}_3 \rangle = \tilde{v}(\vec{k}_2 - \vec{k}_2') \delta(\vec{k}_2 - \vec{k}_2' - \vec{k}_3' + \vec{k}_3) . \quad (8)$$

Equations (7) and (8) correspond to the operators $e^2/\epsilon(r_{13}) r_{13}$ and $e^2/\epsilon(r_{23}) r_{23}$, respectively, where $1/\epsilon(r) r$ is the Fourier transform of $1/\epsilon(q) q^2$ in real space. The valence-band dispersion function $E_v(\vec{k}_3)$ is very anisotropic. If we transform Eq. (5) in real space, the kinetic energy operator for the hole can be written in the following form as introduced by Baldereschi and Lipari[17] (BL) in the limit of strong spin-orbit interaction

$$E_v\left[-\frac{\partial}{\partial \vec{r}_3}\right] = \sigma[-\nabla_3^2 - \tfrac{1}{9}\mu(P^{(2)} \cdot J^{(2)}) + case \tfrac{1}{9}\delta((P^{(2)} \times J^{(2)})_4^{(4)} + \tfrac{1}{5}\sqrt{70}(P^{(2)} \times J^{(2)})_0^{(4)} + (P^{(2)} \times J^{(2)})_{-4}^{(4)})] , \quad (9)$$

where σ is the ratio of electron transverse effective mass to hole effective mass defined as $\sigma \equiv \gamma_1 m_t^*/m_0$ (m_0 is the free-electron mass); $\mu = (6\gamma_3 + 4\gamma_2)/5\gamma_1$ and $\delta = (\gamma_3 - \gamma_2)/\gamma_1$, with γ_1, γ_2, and γ_3 being parameters proposed by Luttinger[18] for the description of the valence-band dispersion relation near the center of the Brillouin zone; $P^{(2)}$ and $J^{(2)}$ are the second-rank symmetric tensors for the linear and angular momentum, respectively, as introduced by BL.[17]

In the limit of strong spin-orbit interaction, the hole wave function transforms according to the double group representations of T_d. We shall label the representations associated with the hole state and the two-electron product state by Γ_h and Γ_e, respectively. The basis wave functions which have overall symmetry $\Gamma^\pm$ can be made by linear combinations of products of two-electron states [of symmetry $(\tau_1\tau_2)\Gamma_e^\pm$] and hole states (of symmetry Γ_h). We shall denote our basis functions as $|mnp[(\tau_1\tau_2)\Gamma_e^\pm \Gamma_h]\Gamma^\pm \mu\rangle$, where the symbol $[(\tau_1\tau_2)\Gamma_e^\pm \Gamma_h]\Gamma^\pm \mu$ indicates how the total-wave-function transforming as the basis vector labeled μ of the overall symmetry $\Gamma^\pm$ is made by the two-electron product states [of symmetry $(\tau_1\tau_2)\Gamma_e^\pm$] and the hole states (of symmetry Γ_h). The indices mn and p represent the remaining quantum numbers for the two electrons and the hole, respectively. The total envelope wave function $B(\vec{k}_1, \vec{k}_2, \vec{k}_3)$ can be expanded in terms of these basis states. The coefficients for expansion, $C(mnp, [(\tau_1\tau_2)\Gamma_e\Gamma_h]\Gamma_\mu^\pm)$ can be determined by the standard configuation-interaction matrix equation,

$$\sum_{\substack{mnp \\ \tau_1\tau_2, \Gamma_e\Gamma_h}} \langle m'n'p'; [(\tau_1'\tau_2')\Gamma_e^{\pm'} \Gamma_h^{\pm'}]\Gamma^\pm \mu | H_{D^0X} | mnp; [(\tau_1\tau_2)\Gamma_e^\pm \Gamma_h]\Gamma^\pm \mu \rangle$$

$$\times C(mnp, [(\tau_1\tau_2)\Gamma_e^\pm \Gamma_h]\Gamma^\pm \mu) = E^{\Gamma^\pm} C(m'n'p', [(\tau_1\tau_2)\Gamma_e^\pm \Gamma_h]\Gamma^\pm \mu) . \quad (10)$$

The Hamiltonian matrix elements for the D^0X involve the matrix elements for the single-particle Hamiltonians, h_e for the two electrons and h_n for the hole, the matrix elements for the electron-electron mutual interaction $v(1,2)$, and the matrix elements for the electron-hole mutual interactions $v(1,3)$ and $v(2,3)$. The matrix elements for h_e and $v(1,2)$ are treated in the same way as in Ref. 11. The electron-electron interaction $v(1,2)$ plays an important role in determining the fine structures in the electronic spectrum of the D^0X. Recalling the results obtained in Ref. 11, we can write

$$\langle m'n'p';[(\tau_1'\tau_2')\Gamma_e'\Gamma_h']\Gamma^{\pm}\mu \mid v(1,2) \mid mnp;[(\tau_1\tau_2)\Gamma_e\Gamma_h]\Gamma^{\pm}\mu\rangle$$
$$\simeq \left[U_0(m'n',mn)\delta_{\tau_1\tau_1'}\delta_{\tau_2\tau_2'}+\sum_{\lambda=1}^{4}U_\lambda(m'n',mn)G_\lambda^{\Gamma_e}(\tau_1\tau_2,\tau_1\tau_2)\right]\delta_{\Gamma_h\Gamma_h'}\delta_{\Gamma_e\Gamma_e'}f_{mn}^{\tau_1\tau_2}f_{m'n'}^{\tau_1'\tau_2'}\pm\cdots, \quad (11)$$

where the ellipsis represents an exchange term and with

$$f_{mn}^{\tau_1\tau_2}\equiv\begin{cases}1/\sqrt{2} & \text{if } m=n \text{ and } \tau_1=\tau_2\\ 1 & \text{otherwise}\end{cases}. \quad (12)$$

U_0 is the intravalley mutual interaction between two electrons with charge distributions along the same axis and (U_0-U_1) represents the intravalley mutual interaction between two electrons with charge distributions along different axes. U_2 and U_3 are the contributions from the momentum-conserving intervalley scattering schemes (longitudinal and transverse). U_4 is the contribution from momentum-nonconserving intervalley scattering schemes. For Ge, there is no U_2 term. The exchange term is obtained from the direct term by exchanging the roles of the two electrons in the final state. The G matrices describing the electron-electron couplings are given in Tables V and VI of Ref. 11 for Si and Ge, respectively. As will be shown in Sec. III, the net contribution from the U_1, U_2, U_3, and U_4 term is less than 5% of the total energy. In the zeroth-order approximation, the terms involving U_1, U_2, U_3, and U_4 are neglected. The energy levels can therefore be labeled by the symmetry representation of single-particle states. For Si:P, the ordering of the energy levels for the lowest states of various configurations is (starting from the lowest): $(\Gamma_1\Gamma_1)$, $(\Gamma_1\Gamma_5)$, $(\Gamma_5\Gamma_5)$, $(\Gamma_3\Gamma_5)$, and $(\Gamma_3\Gamma_3)$. For Ge:As, it is $(\Gamma_1\Gamma_1)$, $(\Gamma_1\Gamma_5)$, and $(\Gamma_5\Gamma_5)$. This ordering is mainly determined by the sum of energies in single-particle states as predicted by the shell model.[7] However, the spacing between energy levels of various configurations is much smaller than that between the sum of one-particle energies in donor states belonging to various representations. The matrix elements for h_h are the same as those for an acceptor system except for a reversed sign in the potential energy part. Hence, we can treat them in the same way as in Ref. 17. The electron-hole interaction terms lead to further complication and will be treated in more detail here. In Appendix A, we derive the matrix elements for the electron-hole interaction with the electron states restricted to s-like (ellipsoidal) orbitals and the hole states restricted to s-like and d_0-like orbitals. We obtain a general expression for the electron-hole interaction term

$$\langle m'n'p';[(\tau_1'\tau_2')\Gamma_e^{\pm'}\Gamma_h']\Gamma^{\pm}\mu \mid v(1,3) \mid mnp;[(\tau_1\tau_2)\Gamma_e^{\pm}\Gamma_h]\Gamma^{\pm}\mu\rangle$$
$$=J^{\Gamma}([(\tau_1'\tau_2')\Gamma_e'\Gamma_h'],[(\tau_1\tau_2)\Gamma_e\Gamma_h])V_{13}(m'p',mp)\delta_{\tau_2\tau_2'}\delta_{nn'}f_{mm'}^{\tau_1\tau_1'}f_{nn'}^{\tau_2\tau_2'}\pm\cdots, \quad (13)$$

where the ellipsis represents an exchange term and where $V_{13}(m'p',mp)$ is the matrix for the Coulomb mutual interaction, i.e.,

$$V_{13}(m'p',mp)=\langle m'p' \mid v(1,3) \mid mp\rangle. \quad (14)$$

J^{Γ} represents the electron-hole coupling matrix between states of different configurations but the same overall symmetry, Γ. The exchange term is obtained from the first term by exchanging the roles of the two electrons in the final state. The J matrices depend on the orbital symmetry of the hole states p and p'. For hole states p,p' of the same orbital symmetry (i.e., same angular momentum), all the J matrices are equal to the identity matrix. For hole states p,p' of different orbital symmetries (e.g., one s-like and the other d-like), the J matrices are nontrivial and are listed in Table VI for Si and Table VII for Ge, respectively. It is noticed that all the matrices given in Table VI and Table VII can be diagonalized with the resulting eigenvalues equal to either 1 or -1. This is the same as one would have obtained if the electron in each of the N equivalent valleys had been considered to interact with the hole independently. To illustrate the use of Tables VI and VII, we take the states associated with the configuration $[(15)\Gamma_5\Gamma_8]\Gamma^{\pm}$ in Si as an example. Here, we use (ij) to denote the electronic configuration $(\Gamma_i\Gamma_j)$. The electron-hole interaction coupling an s-like and a d-like hole state can be written as

$$\langle[(15)\Gamma_5\Gamma_8]\Gamma^{\pm} \mid v(13)+v(23) \mid [(15)\Gamma_5\Gamma_8]\Gamma^{\pm}\rangle$$
$$=\{\langle[(15)\Gamma_5\Gamma_8]\Gamma \mid v(13)+v(23) \mid [(15)\Gamma_5\Gamma_8]\Gamma\rangle+\langle[(51)\Gamma_5\Gamma_8]\Gamma \mid v(13)+v(23) \mid [(51)\Gamma_5\Gamma_8]\rangle\}/2, \quad (15)$$

where we have used the relation $[(15)\Gamma_5\Gamma_8]\Gamma^{\pm}=1/\sqrt{2}\{[(15)\Gamma_5\Gamma_8]\Gamma\pm[(51)\Gamma_5\Gamma_8]\Gamma\}$ and the fact that all cross terms vanish as indicated in Table VI. We can write the above matrix elements in terms of J matrices and the electron-hole coupling strength $\bar{V}_{eh}$, where $V_{eh}\equiv 2a_s a_d V_{sd}$. a_s and a_d are the coefficients associated with the s-like and d-like components, respectively, in the hole ground state. V_{sd} is the electron-hole interaction coupling the s-like and d-like components of the hole states with the electron enveloped function centered at a valley along the z axis. We obtain

$$\langle[(15)\Gamma_5\Gamma_8\Gamma^{\pm}\,|\,v(1,3)+v(23)\,|\,[(15)\Gamma_5\Gamma_8]\Gamma^{\pm}\rangle=J^{\Gamma}([(51)\Gamma_5\Gamma_8],[(51)\Gamma_5\Gamma_8])\bar{V}_{eh}\ , \tag{16}$$

which equals $\bar{V}_{eh}$, $-\bar{V}_{eh}$, $\frac{4}{5}\bar{V}_{eh}$, and $-\frac{4}{5}\bar{V}_{eh}$ for $\Gamma=\Gamma_6$, Γ_7, Γ_8, and Γ_8', respectively. Here, $\bar{V}_{eh}$ is the electron-hole coupling strength for a Γ_5-symmetry electron. There is also an off-diagonal term $-\frac{3}{5}\bar{V}_{eh}$ for the coupling between state with $\Gamma=\Gamma_8$ and $\Gamma=\Gamma_8'$. Since the two states are degenerate in the absence of electron-hole interaction, we can simply diagonalize the J-matrix coupling the states $[(51)\Gamma_5\Gamma_8]\Gamma_8$ and $[(51)\Gamma_5\Gamma_8]\Gamma_8'$ and obtain the eigenvalues -1 and 1. We therefore also obtain the values $\bar{V}_{eh}$ and $-\bar{V}_{eh}$ for the two mixed states associated with $\Gamma=\Gamma_8$ and Γ_8', which diagonalize the J matrix. In other words, the initially fourfold-degenerate hole states are now split into two levels (one classified as $\Gamma_6+\Gamma_8$, another classified as $\Gamma_7+\Gamma_8'$) due to the presence of a Γ_5 electron. This is as expected, since the Γ_5 electron in Si only occupies valleys along the same axis and hence produces an electron-hole splitting in the same manner as in a free-exciton system. If we apply this argument to the states associated with the same configuration in Ge, we obtain the values $\bar{V}_{eh}$, $\bar{V}_{eh}$, $-\frac{4}{5}\bar{V}_{eh}$, and $-\frac{1}{5}\bar{V}_{eh}$ for the diagonal terms with $\Gamma=\Gamma_6$, Γ_7, Γ_8, and Γ_8', respectively, and a value $-\frac{2}{5}\bar{V}_{eh}$ for the off-diagonal term of the J-matrix coupling the $\Gamma=\Gamma_8$ and $\Gamma=\Gamma_8'$ states. This J matrix also couples the above two states with the $[(11)\Gamma_1\Gamma_8]\Gamma_8$ state as shown in Table VII. If we neglect the coupling between the $[(11)\Gamma_1\Gamma_8]\Gamma_8$ state and the $[(51)\Gamma_5\Gamma_8]\Gamma_8'$ states (this is approximately valid due to the fact that the energy of the $[(11)\Gamma_1\Gamma_8]\Gamma_8$ state is lower than the $[(51)\Gamma_5\Gamma_8]\Gamma_8$ state by a large value compared to $\bar{V}_{eh}$), we can diagonalize the submatrix which couples the two states of the same electronic symmetry $(51)\Gamma_5$, and obtain the eigenvalues 0 and -1. We therefore conclude that the Γ_5 electron will split the hole state into three almost equally spaced levels with the highest level classified as $\Gamma_6+\Gamma_7$ and the lower two level classified as Γ_8 symmetry. This is particularly interesting because it reflects the fact that the Γ_5 electrons in Si and in Ge are intrinsically different in that the former occupies valleys along the same axis and the latter has the same probability being in valleys along four different axes.

III. CALCULATION METHOD

Our calculation is based on the Hartree-Fock approximation. It is assumed that the fine structure in the excitation spectrum is approximately unaffected by the correlation effect, although this effect plays an important role in the binding of the system. The procedure of our calculation is divided into three steps. In the first step (zeroth-order approximation), both the electron-electron coupling terms (U_1, U_2, U_3, and U_4) and the elctron-hole coupling term ($\bar{V}_{eh}$) are neglected. In the second step, the electron-electron coupling terms are included. In the final step, all coupling terms are included. In the first step, the states of different electronic configurations, denoted as $(\tau_1\tau_2)$, are completely decoupled. We can therefore carry out the calculation for each configuration separately. For convenience, we introduce the normalized units in which distance and energy are measured in units of $\epsilon_0\hbar^2/m_t^* e^2$, the Bohr and $e^4 m_t^*/2\epsilon^2\hbar^2$, the Rydberg. ϵ_0 and m_t^* are the static dielectric constant and the transverse effective mass, respectively.

The Hartree-Fock solutions are expanded in terms of linear combinations of Slater-type orbitals (STO). For each of the two electrons, we use seven s-like basis functions defined by[20]

$$\beta_{nlm}^{\tau\mu}(\vec{r})=\sum_{j=1}^{N}\alpha_j^{\tau}(\mu)e^{i\vec{k}_j\cdot\vec{r}}f_n(r')Y_{lm}(\Omega')\ , \tag{17}$$

where $f_n(r')$ is obtained from the radial part of the STO, $e^{-b_i r'}$; $i=1,\ldots,7$ by the Schmidt othogonalization procedure.[19] These STO are defined in an ellipsoidal coordinate system with eccentricity factor ζ, i.e., with coordinate $\vec{r}'=(x,y,z/\zeta)$. The exponents b_i are given by

$$b_i=b_0/z_i,\quad i=1,\ldots,7$$

with

$$b_0=\begin{cases}2\ \text{bohr}^{-1} & \text{for Si}\\ 4\ \text{bohr}^{-1} & \text{for Ge}\end{cases}$$

and

$$z_i=(1,2,4,8,16,\tfrac{1}{2},\tfrac{1}{4})\ .$$

The eccentricity factor ζ is determined by minimizing the energy expectation value of the effective mass Hamiltonian in the ground-state trial wave function given by Eq. (17) with respect to the exponent. The best value of ζ was found to be 0.57 for Si and 0.355 for Ge.[20] The fact that the ground state in the neutral donor system has very little admixture ($\lesssim 1\%$) of higher angular-momentum state[20] (defined in ellipsoidal coordinates) makes it a good approximation to expand the electron wave function in terms of s-like orbitals.

For the hole, however, the mixing of s-like and d-like orbitals is appreciable, and hence we use seven s-like and seven d-like Slater orbitals defined by[17]

$$\phi_p^{\mu_h}=f_p(r)\,|\,L=l,\ J=\tfrac{3}{2};\ F=\tfrac{3}{2},\ F_z=\mu_h\rangle,\qquad l=0.2\ , \tag{18a}$$

where $\vec{F}\equiv\vec{L}+\vec{J}$, with $\vec{J}$ and $\vec{L}$ denoting the spin and orbital angular momentum for the hole, respectively. The radial part $f_p(r)$ is obtained from seven STO's (in spherical coordinates),

$$g_i(r)=\begin{cases}(4c_i^3)^{1/2}e^{-c_i r} & \text{for } l=0\\ \left[\dfrac{4c_i^5}{3}\right]^{1/2} re^{-c_i r} & \text{for } l=2\end{cases} \tag{18b}$$

by the Schmidt orthogonalization procedure.[19] The exponents c_i are given by $c_i=c_0/z_i$, $i=1,\ldots,7$ with $c_0=0.5$ bohr^{-1} and z_i's being the same as used for the electrons.

In the first step, the expansion coefficients in Eq. (10) are decomposed into the product of three terms, viz.,

$$C(mnp,[(\tau_1\tau_2)\Gamma_e\Gamma_h]\Gamma^{\pm}\mu)=C_{\tau_1}(m)C_{\tau_2}(n)C_{\Gamma_h}(p)\ . \tag{19}$$

Then, Eq. (10) can be simplified to

$$\sum_{mnp}\langle m'n'p'\,|\,H_{D^0X}\,|\,mnp\rangle_{\tau_1\tau_2}C_{\tau_1}(m)C_{\tau_2}(n)C_{\tau_h}(p)=E_0(\tau_1,\tau_2)C_{\tau_1}(m')C_{\tau_2}(n')C_{\tau_h}(p')\ , \tag{20a}$$

where

$$\begin{aligned}\langle m'n'p'\,|\,H_{D^0X}\,|\,mnp\rangle_{\tau_1\tau_2}\equiv{}&{}_{\tau_1}\langle m'\,|\,H^{(1)}\,|\,m\rangle_{\tau_1}\delta_{nn'}\delta_{pp'}+{}_{\tau_2}\langle n'\,|\,H^{(2)}\,|\,n\rangle_{\tau_2}\delta_{pp'}\delta_{mm'}\\ &+{}_{\Gamma_h}\langle p'\,|\,H^{(3)}\,|\,p\rangle_{\Gamma_h}\delta_{mm'}\delta_{nn'}+\langle m'n'\,|\,v(1,2)\,|\,mn\rangle\delta_{pp'}\\ &-\langle m'p'\,|\,v(1,3)\,|\,mp\rangle\delta_{nn'}\delta_{l_3'l_3}-\langle n'p'\,|\,v(2,3)\,|\,np\rangle\delta_{mm'}\delta_{l_3'l_3}\ ,\end{aligned} \tag{20b}$$

with l_3,l_3' indicating the angular momentum quantum number of the hole states. Equation (20a) can be solved for the coefficients $C_{\tau_1}(m)$, $C_{\tau_2}(n)$, and $C_{\tau_3}(p)$ self-consistently by iteration.

In the second step, the correction due to the electron-electron coupling is included. We evaluate the contributions due to the terms U_λ ($\lambda=1,2,3,4$) on the zeroth-order ground-state wave functions obtained in the first step. It is found that, for Ge, the intervalley scattering terms U_3 and U_4 are 2 orders of magnitude smaller than the U_1 term and can be neglected. The zeroth-order ground states of various configurations are now coupled together through the off-diagonal matrix elements of G_λ^Γ's. The sub-Hamiltonians are defined for each symmetry $\Gamma_e^{\pm}$ by[11]

$$H^{\Gamma_e^{\pm}}(\tau_1\tau_2,\tau_1'\tau_2')=E_0(\tau_1,\tau_2)\delta_{\tau_1\tau_1'}\delta_{\tau_2\tau_2'}+\sum_{\lambda=1}^{4}U_\lambda G_\lambda^{\Gamma_e}(\tau_1\tau_2,\tau_1'\tau_2')\pm\sum_{\lambda=1}^{4}U_\lambda^{\text{ex}}G_\lambda^{\Gamma_e}(\tau_1\tau_2,\tau_2'\tau_1')(1-\delta_{\tau_1\tau_1'}\delta_{\tau_2\tau_2'})\ , \tag{21}$$

where U_λ^{ex} is the exchange term associated with U_λ. $E_0(\tau_1\tau_2)$ are the eigenvalues obtained in the zeroth-order approximation. These energy levels except $E_0(\Gamma_1\Gamma_1)$ are now split into several states, each one associated with an irreducible representation of the group T_d. The coupling coefficients between states of different electronic configurations are also obtained. We shall denote the energy eigenvalues of $H^{\Gamma_e^{\pm}}(\tau_1\tau_2,\tau_1'\tau_2')$

as $E_1[(\tau_1\tau_2)\Gamma_e^{\pm}]$. In the final step, the electron-hole coupling term $\bar{V}_{eh}$ is included. As shown in Tables VI and VII this term only couples states separated by an energy large compared to $\bar{V}_{eh}$ or states associated with the same electronic configuration. For the former case, the coupling can be neglected. For the latter case, the zeroth-order energies are degenerate. If we diagonalize the submatrices which couple states associated with the same electronic configurations, we obtain the eignvalues -1 and 1 for most of them, the others being between -1 and 1. We therefore repeat the Hartree-Fock calculations for each electronic configuration $(\tau_1\tau_2)$ with the J matrices set equal to 1 and -1. The contributions of $\bar{V}_{eh}$ to the Hamiltonian matrix when the J coefficients are between -1 and 1 can be obtained simply by interpolation.

We have expanded the hole wave function in terms of s-like and d-like orbitals (with total angular momentum $F \equiv L + J = \frac{3}{2}$). Therefore, the contributions due to the other orbitals (e.g., with $L=2$ and $F=\frac{7}{2}, \frac{5}{2}, \frac{1}{2}$, and $L=4,6,\ldots$, etc.,[21] are not included. For simplicity, we will include the correction due to these orbitals by multiplying the values of $\bar{V}_{eh}$ obtained above by a correction factor f_c, where f_c is the ratio of the electron-hole splitting for the free exciton system obtained with and without these orbitals. For this purpose, we have calculated the ground-state splitting of the free exciton for Si and Ge, using the basis set given by Eqs. (18). We obtain a value for the splitting 0.58 meV for Ge and 0.92 meV for Si. Comparing our results with the accurate results obtained by Lipari and Altarelli,[21,22] we obtain that $f_c \simeq 2$ and 0.5 for Ge and Si, respectively.

The remaining task is to diagonalize the sub-Hamiltonian defined by

$$H^{\Gamma^{\pm}}((\tau_1\tau_2)\Gamma_e\Gamma_8,(\tau_1\tau_2)\Gamma_e'\Gamma_8) = E_1((\tau_1\tau_2)\Gamma_e^{\pm})\delta_{\Gamma_e\Gamma_e'} + \bar{V}_{eh}J^{\Gamma}([(\tau_1\tau_2)\Gamma_e\Gamma_8],[(\tau_1\tau_2)\Gamma_e'\Gamma_8]) + \bar{V}_{eh}'J^{\Gamma}([(\tau_2\tau_1)\Gamma_e\Gamma_8],[(\tau_2\tau_1)(\Gamma_e'\Gamma_8]) , \quad (22)$$

where $E_1((\tau_1\tau_2)\Gamma_e^{\pm})$ is the eigenvalue of $H^{\Gamma_e^{\pm}}(\tau_1\tau_2,\tau_1'\tau_2')$ obtained in the previous step. $\bar{V}_{eh}$ and $\bar{V}_{eh}'$ are the electron-hole coupling strengths associated with the τ_1- and τ_2-symmetry electrons, respectively. The final results for the energy eigenvalues will be denoted as $E((\tau_1\tau_2)\Gamma_e^{\pm}\Gamma_8]\Gamma^{\pm})$.

IV. RESULTS AND DISCUSSION

We will discuss our results for Si and Ge separately.

A. Si

Tables I–IV show the ground-state energies for various configurations obtained in three steps (denoted by E_0, E_1, and E, respectively) for Si doped by the impurities P, As, Sb, and Li, respectively. For illustration, the theoretical spectrum for Si:P is plotted in Fig. 1, showing the systematic change of the energy levels in various approximations. The smallness of the fine-structure splitting, as compared to the total-binding energies, justifies the validity of the first-order approximation used to evaluate the various fine-structure terms. For example, for the $(\Gamma_1\Gamma_5)$ states in Si:P, we have $\bar{V}_{eh} \simeq U_2 \simeq U_3 = \frac{1}{5}U_1 \simeq \frac{1}{500}E_0(\Gamma_1\Gamma_5)$. As shown in Fig. 1, when the electron-electron and electron-hole coupling terms are neglected, we obtain one energy level for each configuration and the ordering is the same as predicted by the shell model.[7] When the electron-electron coupling (dominated by U_1 is included, all levels except the $(\Gamma_1\Gamma_1)$ state are split into several states. We find that the mixing of configuration is appreciable only for states of the same overall symmetry and close in energy. The admixture of $(\Gamma_3\Gamma_3)\Gamma_1^+$ and $(\Gamma_5\Gamma_5)\Gamma_1^+$ in the ground state $(\Gamma_1\Gamma_1)\Gamma_1^+$ is less than 0.1%, whereas the mixing between $(\Gamma_3\Gamma_3)\Gamma_1^+$ and $(\Gamma_5\Gamma_5)\Gamma_1^+$ states is substantial (about 9%). The $(\Gamma_3\Gamma_3)\Gamma_3^+$ state also couples strongly with the $(\Gamma_5\Gamma_5)\Gamma_3^+$ state (about 8% mixing). The remaining states only couple with each other weakly (less than 1%). When the electron-hole coupling is included, the states are split further, and mixing is only important between states associated with the same electronic configuration. The splitting due to the electron-hole coupling is an order of magnitude smaller than the splitting due to the electron-electron coupling and difficult to observe experimentally. It should be noted that the results presented here are slightly different (by about 1%) than the results presented previously.[12] In the present calculation, we have adjusted the empirical parameters, J_λ for the short-range core potentials[11] so that the use of a restricted basis set (consisting of seven s-like ellipsoidal STO) can reproduce the experimental values for the binding energies for the low-lying donor states. In the previous calculation, we did not make this adjustment and did not include the $\vec{q}$ dependence of the dielectric function

TABLE I. Total energies of the lowest-lying states of various configurations of the D^0X calculated in three steps (E_0, E_1, and E) for Si:P. All energies are in meV. The notation $\Gamma_e^{\pm}$ in the fourth column stands for the irreducible representation to which the two-electron product wave function belongs; $\pm$ indicates a spin singlet or triplet.

Material	First step Configuration	E_0	Second step $\Gamma_e^{\pm}$	E_1	Final E Γ_6	Γ_7	Γ_8	Γ_8'
Si:P	$\{\Gamma_3\Gamma_3;\Gamma_8\}$	−42.59	Γ_1^+	−42.58			−42.57	
			Γ_3^+	−42.89	−42.89	−42.89	−42.90	
			Γ_2^-	−43.25				−43.25
	$\{\Gamma_3\Gamma_5;\Gamma_8\}$	−43.39	Γ_5^+	−43.16	−43.21	−43.12	−43.12	−43.12
			Γ_4^-	−43.96	−43.94	−43.97	−43.97	−43.95
			Γ_4^+	−44.04	−44.03	−44.06	−44.06	−44.03
			Γ_5^-	−44.06	−44.11	−44.02	−44.11	−44.02
	$\{\Gamma_5\Gamma_5;\Gamma_8\}$	−44.09	Γ_1^+	−44.08			−44.04	
			Γ_3^+	−44.16	−44.10	−44.23	−44.20	
			Γ_5^+	−44.67	−44.64	−44.71	−44.71	−44.64
			Γ_4^-	−44.76	−44.80	−44.73	−44.8-	−44.73
	$\{\Gamma_1\Gamma_3;\Gamma_8\}$	−53.00	Γ_3^+	−53.13	−53.09	−53.17	−53.13	
			Γ_3^-	−53.35	−53.31	−53.39	−53.35	
	$\{\Gamma_1\Gamma_5;\Gamma_8\}$	−53.22	Γ_5^+	−53.34	−53.38	−53.30	−53.38	−53.30
			Γ_5^-	−53.64	−53.68	−53.60	−53.68	−53.60
	$\{\Gamma_1\Gamma_1;\Gamma_8\}$	−57.36	Γ_1^+	−57.67			57.67	

TABLE II. Total energies of the lowest-lying states of various configurations of the D^0X, calculated in three steps (E_0, E_1, and E) for Si:As.

Material	First step Configuration	E_0	Second step $\Gamma_e^{\pm}$	E_1	Final E Γ_6	Γ_7	Γ_8	Γ_8'
Si:As	$\{\Gamma_3\Gamma_3;\Gamma_8\}$	−41.09	Γ_1^+	−41.09			−41.08	
			Γ_3^+	−41.39	−41.39	−41.39	−41.40	
			Γ_2^-	−41.72				−41.72
	$\{\Gamma_3\Gamma_5;\Gamma_8\}$	−41.92	Γ_5^+	−41.71	−41.76	−41.76	−41.75	−41.68
			Γ_4^-	−42.48	−42.47	−42.29	−42.29	−42.47
			Γ_4^+	−42.55	−42.54	−42.57	−42.56	−42.54
			Γ_5^-	−42.57	−42.62	−42.54	−42.61	−42.54
	$\{\Gamma_5\Gamma_5;\Gamma_8\}$	−42.65	Γ_1^+	−42.65			−42.61	
			Γ_3^+	−42.73	−42.67	−42.80	−42.77	
			Γ_5^+	−43.22	−42.19	−43.25	−43.25	−43.19
			Γ_4^-	−43.30	−43.33	−43.27	−43.33	−43.27
	$\{\Gamma_1\Gamma_3;\Gamma_8\}$	−60.69	Γ_3^+	−60.76	−60.72	−60.80	−60.76	
			Γ_3^-	−60.91	−60.87	−60.95	−60.91	
	$\{\Gamma_1\Gamma_5;\Gamma_8\}$	−60.82	Γ_5^+	−60.88	−60.92	−60.84	−60.92	−60.84
			Γ_5^-	−61.07	−61.11	−61.03	−61.11	−61.03
	$\{\Gamma_1\Gamma_1;\Gamma_8\}$	−66.65	Γ_1^+	−66.87			−66.87	

TABLE III. Total energies of the lowest-lying states of various configurations of the D^0X, calculated in three steps (E_0, E_1, and E) for Si:Sb.

Material	First step Configuration	E_0	Second step $\Gamma_e^{\pm}$	E_1	Final E Γ_6	Γ_7	Γ_8	Γ_8'
Si:Sb	$\{\Gamma_3\Gamma_3;\Gamma_8\}$	−40.28	Γ_1^+	−40.33			−40.32	
			Γ_3^+	−40.61	−40.61	−40.61	−40.62	
			Γ_2^-	−40.89				−40.89
	$\{\Gamma_5\Gamma_5;\Gamma_8\}$	−42.96	Γ_5^+	−41.57	−41.61	−41.53	−41.61	−41.53
			Γ_4^-	−42.32	−42.31	−42.33	−42.33	−42.31
			Γ_4^+	−42.39	−42.38	−42.40	−42.40	−42.38
			Γ_5^-	−42.40	−42.44	−42.37	−42.44	−42.37
			Γ_1^+	−42.91			−42.88	
			Γ_3^+	−42.99	−42.93	−43.05	−43.02	
			Γ_5^+	−43.53	−43.50	−43.56	−43.56	−43.50
			Γ_4^-	−43.62	−43.65	−43.59	−43.65	−43.59
	$\{\Gamma_1\Gamma_3;\Gamma_8\}$	−50.11	Γ_3^+	−50.25	−50.21	−50.29	−50.25	
			Γ_3^-	−50.46	−50.42	−50.50	−50.46	
	$\{\Gamma_1\Gamma_5;\Gamma_8\}$	−50.54	Γ_5^+	−50.67	−50.71	−50.63	−50.71	−50.63
			Γ_5^-	−50.99	−51.03	−50.96	−51.03	−50.96
	$\{\Gamma_1\Gamma_1;\Gamma_8\}$	−54.25	Γ_1^+	−54.48			−54.58	

TABLE IV. Total energies of the lowest-lying states of various configurations of the D^0X, calculated in three steps (E_0, E_1 and E) for Si:Li.

Material	First step Configuration	E_0	Second step $\Gamma_e^{\pm}$	E_1	Final E Γ_6	Γ_7	Γ_8	Γ_8'
Si:Li	$\{\Gamma_3\Gamma_3;\Gamma_8\}$	−43.01	Γ_1^+	−43.47			−43.46	
			Γ_3^+	−43.68	−43.68	−43.68	−43.69	
			Γ_2^-	−43.67				−43.67
	$\{\Gamma_3\Gamma_5;\Gamma_8\}$	−41.79	Γ_5^+	−43.22	−43.27	−43.17	−43.27	−43.17
	$\{\Gamma_3\Gamma_5;\Gamma_8\}$	−43.06	Γ_4^-	−43.63	−43.61	−43.64	−43.64	−43.61
			Γ_4^+	−43.72	−43.70	−43.74	−43.74	−43.70
			Γ_5^-	−43.73	−43.78	−43.69	−43.78	−43.69
	$\{\Gamma_5\Gamma_5;\Gamma_8\}$	−43.10	Γ_1^+	−42.79			−42.78	
			Γ_3^+	−43.13	−43.07	−43.20	−43.14	
			Γ_5^+	−43.68	−43.65	−43.71	−43.71	−43.65
			Γ_4^-	−43.76	−43.79	−43.73	−43.79	−43.72
	$\{\Gamma_1\Gamma_3;\Gamma_8\}$	−42.23	Γ_3^+	−42.13	−42.10	−42.16	−42.13	
			Γ_3^-	−42.85	−42.82	−42.88	−42.85	
	$\{\Gamma_1\Gamma_5;\Gamma_8\}$	−42.27	Γ_5^+	−42.06	−42.09	−42.03	−42.09	−42.03
			Γ_5^-	−42.90	−42.93	−42.87	−42.93	−42.87
	$\{\Gamma_1\Gamma_1;\Gamma_8\}$	−41.25	Γ_1^+	−41.44			−41.44	

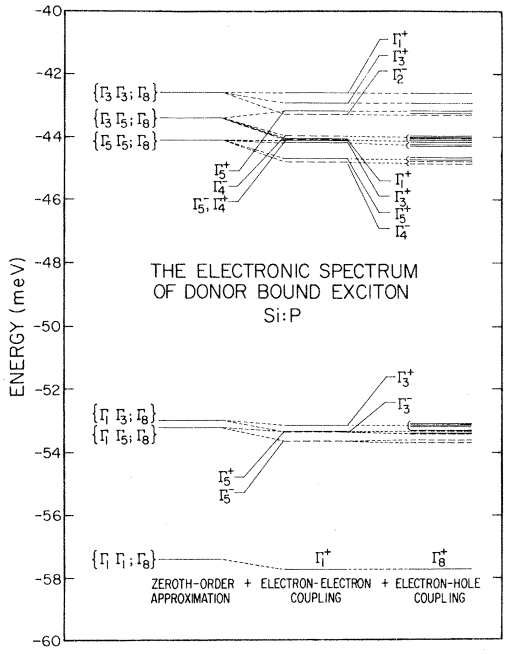

FIG. 1. Theoretical electronic spectrum for D^0X in Si:P plotted in three consecutive steps: zeroth-order approximation (ZOA), ZOA plus electron-electron coupling, and ZOA plus all coupling terms. The notations for the symmetry labels are defined in the text.

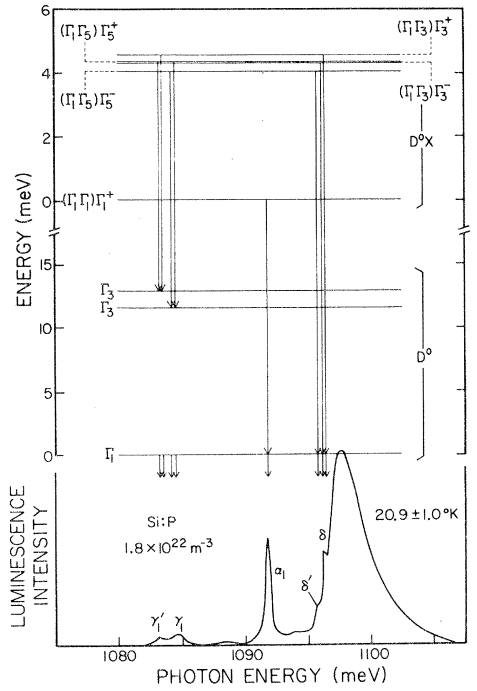

FIG. 2. Theoretically predicted transition lines (indicated by arrows) plotted accompanied with the experimental data for D^0X in Si:P. The symmetry labels of the type $(\Gamma\Gamma')\Gamma_e$ represent a state associated with the configuration $\{\Gamma\Gamma';\Gamma_8\}$ with $\Gamma_e^{\pm}$ denoting the symmetry of the two-electron product states. + (−) indicate a spin singlet (triplet) state. The data are taken from Lightowlers *et al.* (Ref. 23).

for the intravalley mutual interaction terms. However, there is no qualitative difference between these two calculations.

To compare our theoretical results with the experimental data, we have plotted the energy-level scheme obtained in the second step (zeroth-order approximation plus the electron-electron coupling) for D^0X and D^0 in Si:P in Fig. 2, along with the experimental data obtained by Lightowlers *et al.*[23] The fine-structure splittings due to the electron-hole coupling are not shown here, since they are too small to be resolved experimentally (see Fig. 1). All possible optical transitions are indicated by arrows. The whole excitation spectrum has been shifted by a uniform correlation energy. As shown in this figure, the agreement between theory and experiment is very good. All the peaks except the α_1 line observed in the luminescence data are a superposition of several lines. Our theoretical spectrum predicts a line due to the optical transition from the $(\Gamma_1\Gamma_5)\Gamma_5^-$ state of D^0X to the Γ_5 state of D^0 at approximately the same energy position of the δ' line. This line was first observed by Thewalt[24] and cannot be explained by the shell model. For Si:As and Si:Sb, similar theoretical spectra can be obtained using Tables II and III, and are again in good agreement with the experimental data. For Si:As, the energy spacings between the group of states associated with the $(\Gamma_1\Gamma_3)$ and $(\Gamma_1\Gamma_5)$ configurations and the ground state obtained in the present calculation are about 1.5 meV larger than the experimental value for the spacing between the δ line and the α_1 line. On the other hand, by looking at the optical transitions from the $(\Gamma_1\Gamma_3)$ and $(\Gamma_1\Gamma_5)D^0X$ excited states to the Γ_3 and Γ_5 donor excited states (γ lines), Elliott *et al.*[25] have obtained a value of $\simeq$5.8 meV for the energy separation between the $(\Gamma_1\Gamma_3)$ and $(\Gamma_1\Gamma_5)$ excited states and the ground state in Si:As. This value is in good agreement with the present calculation. We therefore attribute the δ line[23] observed in Si:As to the optical transition involving a p-like hole excited state.

For Li, an interstitial donor in Si, the energy spectrum is qualitatively different than that for the other donors (substitutional). The major difference is that in Si:Li, the ordering for the donors states are inverted, i.e., the Γ_3 and Γ_5 states have lower energies than the Γ_1 state.[26] In the upper part of Fig. 3, we plot our theoretical spectrum for D^0X in

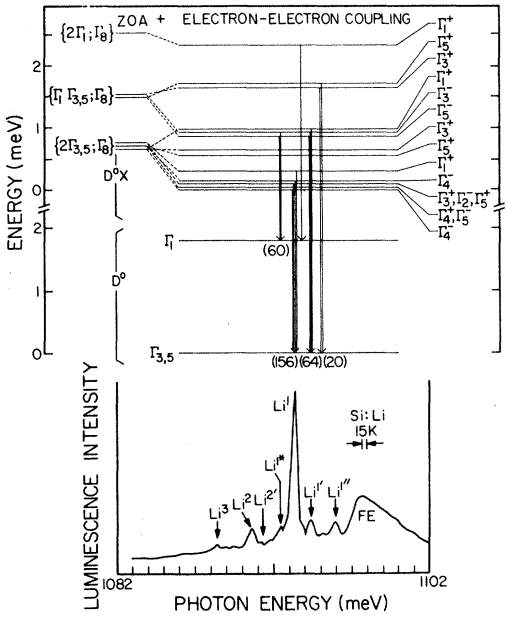

FIG. 3. Theoretical electronic spectrum in Si:Li plotted in two steps: zeroth-order approximation (ZOA), ZOA plus electron-electron coupling. The energy-level scheme for the neutral donor is plotted in the middle panel (after Ref. 26). Theoretically predicted transition lines are indicated by arrows. The experimental data taken from Thewalt (Ref. 27) are plotted in the bottom panel for comparison.

Si:Li, showing the systematic change for energy levels obtained in the zeroth-order approximation (ZOA) and ZOA plus electron-electron coupling. As shown in this figure, in the zeroth-order approximation, the states $\{2\Gamma_5;\Gamma_8\}$ and $\{2\Gamma_3;\Gamma_8\}$ are nearly degenerate, so are the states $\{\Gamma_1\Gamma_5;\Gamma_8\}$ and $\{\Gamma_1\Gamma_3;\Gamma_8\}$. This is expected, since the Γ_3 and Γ_5 donor states in Si:Li are nearly degenerate. When the electron-electron coupling term is included, these levels split into a group of states whose energy spreading is approximately 1 meV. To compare with the experimental data, we plot the energy level scheme for the D^0 in the middle of Fig. 3 and the experimental spectrum obtained by Thewalt at the bottom of Fig. 3. The possible optical transitions are indicated by arrows. The whole spectrum is shifted by the correlation energy of about 7.3 meV. The number of nearly degenerate states associated with a line is indicated in parentheses. It is found that the main bound exciton line, marked Li^1, corresponds to the transition from a group of 156 states associated with the configuration $\{2\Gamma_{3,5};\Gamma_8\}$ and a group of 60 states associated with the configuration $\{\Gamma_1\Gamma_{3,5};\Gamma_8\}$ (plus 4 states associated with the configuration $\{2\Gamma_{3,5};\Gamma_8\}$), respectively, to the $\Gamma_{3,5}$ donor ground state. The line marked Li^{1*} corresponds to the transition from a group of 60 states associated with the configuration $\{\Gamma_1\Gamma_{3,5};\Gamma_8\}$ to the Γ_1 excited donor state. There is a small hump between the lines marked $Li^{1'}$ and $Li^{1''}$, which may correspond to the transition from a group of 20 states associated with the $\{\Gamma_1\Gamma_{3,5};\Gamma_8\}$ configuration (which are separated from the gound states by approximately 1 meV) to the donor ground state. This point has to be examined by further experiment. The line marked $Li^{1''}$ cannot be identified with any transitions from an electronic excited state obtained in the present calculation and therefore is attributed to the transition from a hole excited state as proposed by several authors.[27–29]

We can estimate the correlation energy for the ground state by taking the difference between the experimental and the theoretical value for the dissociation energy. The theoretical dissociation energy is obtained by subtracting the binding energy for the neutral donor and for the free exciton from the total binding energy for the donor bound exciton. The binding energy for the neutral donors are 45.5, 53.7, 42.7, and 33.0 meV for Si:P,[30] Si:As,[30] Si:Sb,[30] and Si:Li,[26] respectively. The binding energy for the free exciton is about 14.7 meV.[31] Combining these results with the Hartree-Fock calculation for the total energy, we obtain the dissociation energies −2.5, −1.5, −2.8, and −3.9 meV for Si:P, Si:As, Si:Sb, and Si:Li, respectively. The negative values of the dissociation energy indicated that the system is not bound in the Hartree-Fock approximation. The experimental value for the dissociation energy is about 4.5, 5.5, 4.2, and 3.6 meV for Si:P,[24] Si:As,[23] Si:Sb,[23], and Si:Li,[28] respectively. Taking the difference between the experimental and theoretical values for the dissociation energy, we obtain approximately the same correlation energy, 7 meV for Si doped with P, As, and Sb, and 7.3 meV for Li. In a previous calculation for the ground-state energy of bound excitons in a spherical model,[32] we obtained a correlation energy about 0.2 Ry for an electron-to-hole mass ratio of about 1. Taking a Rydberg to be the binding energy of the donor in Si (31.2 meV) calculated in the Kohn-Luttinger effective mass approximation (EMA),[33] we obtain a correlation energy 6.3 meV, which is in reasonably good agreement with the value estimated from comparing our Hartree-Fock calculation with the experimental data for practical systems.

TABLE V. Total energies of the lowest-lying states of various configurations, calculated in three steps (E_0, E_1, and E) for Ge:P, Ge:As, and Ge:Sb. All energies are in meV.

Material	First step Configuration	E_0	Second step $\Gamma_e^{\pm}$	E_1	Final E Γ_6	Γ_7	Γ_8	Γ_8'
Ge:P	$\{\Gamma_5\Gamma_5;\Gamma_8\}$	−13.07	Γ_1^+	−13.18			−13.07	
			Γ_5^+	−13.28	−13.25	−13.35	−13.18	−13.19
			Γ_3^+	−13.53	−13.56	−13.56	−13.55	
			Γ_4^-	−13.53	−13.44	−13.44	−13.63	−13.53
	$\{\Gamma_1\Gamma_5;\Gamma_8\}$	−15.19	Γ_5^+	−15.37	−15.49	−15.49	−15.26	−15.37
			Γ_5^-	−15.52	−15.64	−15.64	−15.41	−15.52
	$\{\Gamma_1\Gamma_1;\Gamma_8\}$	−16.20	Γ_1^+	−16.62			−16.62	
Ge:As	$\{\Gamma_5\Gamma_5;\Gamma_8\}$	−12.94	Γ_1^+	−13.04			−12.94	
			Γ_5^+	−13.16	−13.22	−13.22	−13.06	−13.26
			Γ_3^+	−13.40	−13.43	−13.43	−13.42	
			Γ_4^-	−13.40	−13.31	−13.31	−13.50	−13.40
	$\{\Gamma_1\Gamma_5;\Gamma_8\}$	−16.34	Γ_5^+	−16.48	−16.60	−16.60	−16.36	−16.48
			Γ_5^-	−16.60	−16.72	−16.72	−16.49	−16.60
	$\{\Gamma_1\Gamma_1;\Gamma_8\}$	−17.61	Γ_1^+	−18.05			−18.05	
Ge:Sb	$\{\Gamma_5\Gamma_5;\Gamma_8\}$	−12.94	Γ_1^+	−12.99			−12.85	
			Γ_5^+	−13.01	−13.09	−13.09	−12.91	−13.15
			Γ_3^+	−13.40	−13.42	−13.42	−13.41	
			Γ_5^-	−13.40	−13.31	−13.31	−13.50	−13.40
	$\{\Gamma_1\Gamma_5;\Gamma_8\}$	−13.10	Γ_5^+	−13.50	−13.60	−13.41	−13.41	−13.50
			Γ_5^-	−13.57	−13.67	−13.67	−13.48	−13.57
	$\{\Gamma_1\Gamma_1;\Gamma_8\}$	−13.25	Γ_1^+	−13.67			−13.67	

B. Ge

In Table V the ground-state energies obtained in three steps [denoted by E_0, E_1, and E for the zeroth-order approximation (ZOA), (ZOA) plus electron-electron coupling, and ZOA plus all coupling terms, respectively] for various configurations are listed for Ge:P, Ge:As, and Ge:Sb. The theoretical spectrum for Ge:P showing the systematic change for the energy levels in various steps is plotted in Fig. 4. Again, it is found that the electron-electron and electron-hole coupling terms are small compared to the total binding energy. For example, for the $(\Gamma_1\Gamma_5)$ states in Ge:P, we have $\bar{V}_{eh}\simeq 20U_3\simeq 20U_4\simeq\frac{1}{3}U_1\simeq\frac{1}{100}E_0(\Gamma_1\Gamma_5)$. The terms U_3 and U_4 are negligibly small, and have been completely ignored in our calculation. The spectrum of Ge is relatively simpler than Si. The electron-electron coupling is very small compared to the energy separation. The mixing between the $(\Gamma_1\Gamma_1)\Gamma_1^+$ state and the $(\Gamma_5\Gamma_5)\Gamma_5^+$ state is about 0.38%. There is no mixing between the other states shown in this figure. The further splitting due to the electron-hole coupling is explicitly shown in this figure. Again, only mixing between states associated with the same electronic configuration is included. The splitting due to the electron-hole coupling is found to be comparable to the splitting due to the electron-electron coupling, and can be observed experimentally. To compare our results with the experimental data, we have plotted the energy-level scheme and the theoretical spectrum in Fig. 5 for Ge:P and in Fig. 6 for Ge:As, accompanied with the experimental spectra obtained by Mayer and Lightowlers.[10] The whole theoretical spectrum is shifted by a correlation en-

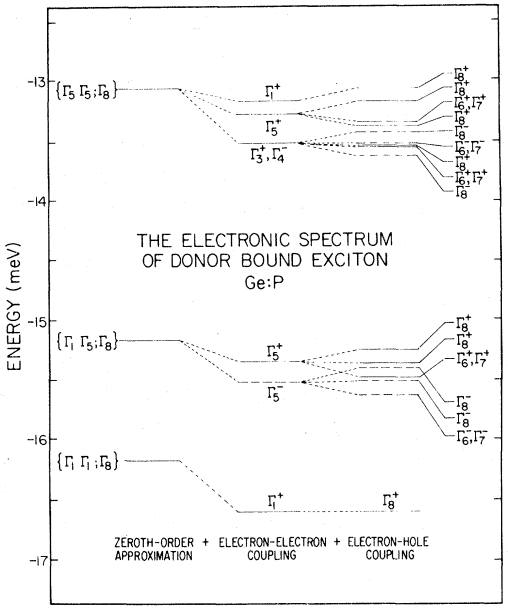

FIG. 4. Theoretical electronic spectrum of donor bound excitons in Ge:P plotted in three steps: zeroth-order approximation (ZOA), ZOA plus electron-electron coupling, and ZOA plus are coupling terms. The notations for symmetry labels are defined in the text.

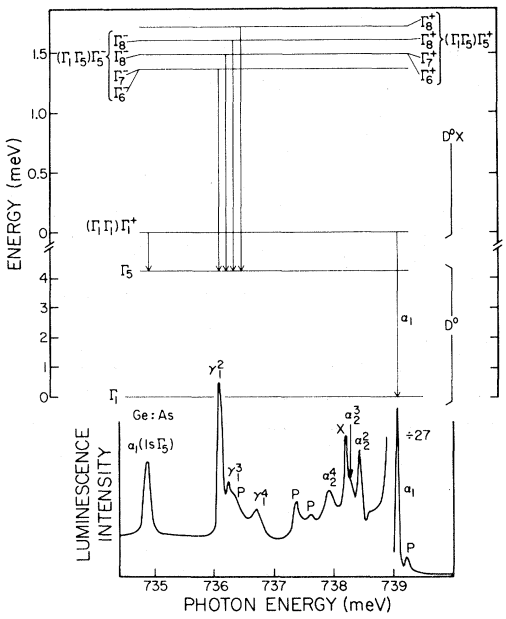

FIG. 6. Theoretical spectrum of optical transitions from D^0X for Ge:As, plotted accompanied with the experimental luminescence spectrum. The theoretically predicted transitions are indicated by arrows. The data are taken from Mayer *et al.* (Ref. 10).

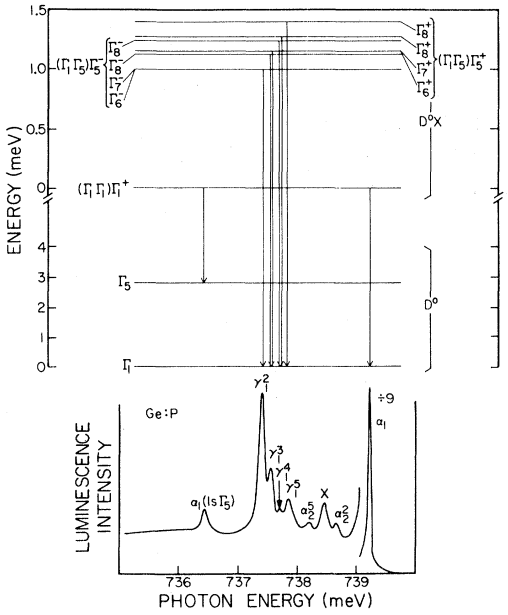

FIG. 5. Theoretical spectrum of the optical transition from donor bound exciton to neutral donor in Ge:P plotted accompanied with the experimental luminenscence spectrum. The theoretical predicted transitions are indicated by arrows. The data are taekn from Mayer *et al.* (Ref. 10).

ergy (of about 1.7 meV) so that the main bound exciton line matches with experimental results (the α_1 line). With this assignment, the theoretical spectrum agrees with the experimental data quite well. The spacing between the first excited state and the ground state agrees with the experimental value for the separation between the α_1 and γ_1^2 line within 0.05 meV. In the phonon-assisted absorption spectrum obtained by Henry and Lightowlers, a line labeled δ^1(LA) is observed, which is due to the transition from the ground state of the neutral donor to the first excited state of the bound exciton. The position of this excited state is about 0.2 meV for Ge:P and 0.45 meV for Ge:As below the lowest electronic excited state obtained in our calculation. Since the no-phonon transitions from this state to the donor Γ_5 state are not observed, we attribute this state to the first hole-excited state (denote as $2P_{3/2}$) in the donor bound-exciton system. The no-phonon transition between the ground state and this $2P_{3/2}$ hole-excited state is forbidden, because the overlap of the electron and hole envelope function vanishes according to symmetry. This fact has recently been confirmed experimentally by Mayer and Lightowlers.[34]

We can also estimate the correlation energy in the same way as we did for Si. The binding energies for the neutral donor are 12.72, 13.87, and

10.3 meV for Ge:P, Ge:As, and Ge:Sb,[35] respectively. The binding energy for the free exciton is about 4.15 meV.[36] Accordingly, we obtain the dissociation energy -0.43, -0.30, and -0.78 meV for Ge:P, Ge:As, and Ge:Sb, respectively. The experimental value for the dissociation energy for Ge:P and Ge:As are 1.3 and 1.45 meV, respectively.[10] Thus we obtain a correlation energy about 1.73 meV for Ge:P and 1.75 meV for Ge:As. Using the result from our previous calculation in a spherical model[32] and taking a Rydberg to be 9.8 meV (the binding energy calculated in EMA[33]), we obtain a correlation energy 1.96 meV for the bound exciton with electron-to-hole mass ratio equal to 1. This is again in reasonable agreement with the value estimated above for a practical system.

V. CONCLUSION

We have developed the theory for the fine structure in the excitation spectrum of donor bound excitons for Si and Ge doped by various impurities. This fine structure is produced mainly by the valley-orbit interaction for the two electrons and the splitting due to the electron-hole interaction. This theory allow us to go beyond the shell model and interpret the detailed structure of the spectrum for donor bound excitons observed in Si and Ge doped with most impurities. Using the energy eigenvalues calculated in the Hartree-Fock approximation, we obtain the theoretical excitation spectrum in good agreement with the available experimental data. Therefore, we conclude that the correlation energy has little effect on the energy differences between the low-lying electronic excited states discussed here and the ground state, although it is important in determining the binding energy. The present work has provided a better understanding for the electronic properties of excitons bound to neutral donors in multivalley semiconductors. The present theory can be also applied to donor bound excitons in GaP with proper treatment of the camel's back structure appearing in the conduction band. This application will be discussed in a future publication.

ACKNOWLEDGMENTS

We gratefully acknowledge D. L. Smith, K. R. Elliott, and C. Mailhiot for numerous discussions. We would like to thank E. C. Lightowlers for sending us a copy of unpublished work. The work was supported in part by the Office of Naval Research under Contract No. N00014-75-C-0423.

APPENDIX A: MATRIX ELEMENTS FOR ELECTRON-HOLE INTERACTION

In this appendix we derive an expression for the matrix elements for the electron-hole interaction in D^0X. The electron states are restricted to s-like (defined in an ellipsoidal coordinate system) orbitals and the hole states restricted to s-like and d-like (in a spherical coordinate system) orbitals. The single-particle basis wave functions for the hole are chosen to be eigenstates of the total angular momentum defined as

$$\vec{F}=\vec{J}+\vec{L}\,,$$

where $\vec{J}$ is the spin and $\vec{L}$ is the orbital angular momentum of the hole. For the ground state (of Γ_8 symmetry), the s-like and d-like orbitals give the most important contribution to the expansion. These basis functions are denoted by

$$\phi_p^{\mu_h}\equiv f_p(r_3)\,|\,0,\tfrac{3}{2};\tfrac{3}{2},\mu_h\rangle \quad \text{or} \quad f_p(r_3)\,|\,2,\tfrac{3}{2};\tfrac{3}{2},\mu_h\rangle\,, \tag{A1}$$

where

$$|\,0,\tfrac{3}{2};\tfrac{3}{2},\mu_h\rangle = Y_{00}(\Omega_3)\chi_{\mu_h},\quad \mu_h=\pm\tfrac{3}{2},\pm\tfrac{1}{2}$$

$$|\,2,\tfrac{3}{2};\tfrac{3}{2},\pm\tfrac{3}{2}\rangle = \frac{1}{\sqrt{5}}Y_{20}(\Omega_3)\chi_{\pm 3/2}-\sqrt{2/5}[Y_{2\pm1}(\Omega_3)\chi_{\pm1/2}-Y_{2\pm2}(\Omega_3)\chi_{\mp1/2}]\,,$$

and

$$|\,2,\tfrac{3}{2};\tfrac{3}{2},\pm\tfrac{1}{2}\rangle = \frac{-1}{\sqrt{5}}Y_{20}(\Omega_3)\chi_{\pm1/2}+\sqrt{2/5}[Y_{2\pm2}(\Omega_3)\chi_{\mp3/2}+Y_{2\mp1}(\Omega_3)\chi_{\pm3/2}]\,,$$

with χ_{μ_h} being the spin-$\frac{3}{2}$ spinor.

TABLE VI. Coupling matrices $J^{\Gamma}((\tau_1'\tau_2')\Gamma_e'\Gamma_8,(\tau_1\tau_2)\Gamma_e\Gamma_8)$ of the electron-hole interaction $v(1,3)$ calculated for Si; the states in various configurations $[(\Gamma_i\Gamma_j)\Gamma_e,\Gamma_8]$ are denoted by the simplified notation $(ij)\Gamma_e$.[a]

J^{Γ_6}	$(31)\Gamma_3$
$(31)\Gamma_3$	-1

J^{Γ_6}	$(51)\Gamma_5$
$(51)\Gamma_5$	1

J^{Γ_6}	$(53)\Gamma_4$
$(53)\Gamma_4$	-1

J^{Γ_6}	$(53)\Gamma_5$
$(53)\Gamma_5$	1

J^{Γ_6}	$(55)\Gamma_3$
$(55)\Gamma_3$	-1

J^{Γ_6}	$(13)\Gamma_3$	$(33)\Gamma_3$
$(13)\Gamma_3$	0	1
$(33)\Gamma_3$	1	0

J^{Γ_6}	$(55)\Gamma_4$	$(55)\Gamma_5$
$(55)\Gamma_4$	$\frac{1}{2}$	$-\sqrt{3}/2$
$(55)\Gamma_5$		$-\frac{1}{2}$

J^{Γ_6}	$(15)\Gamma_5$	$(35)\Gamma_5$	$(35)\Gamma_4$
$(15)\Gamma_5$	0	$1/\sqrt{2}$	$1/\sqrt{2}$
$(35)\Gamma_5$		$\frac{1}{2}$	$-\frac{1}{2}$
$(35)\Gamma_4$			$\frac{1}{2}$

J^{Γ_7}	$(31)\Gamma_3$
$(31)\Gamma_3$	1

J^{Γ_7}	$(51)\Gamma_5$
$(51)\Gamma_5$	-1

J^{Γ_7}	$(53)\Gamma_4$
$(53)\Gamma_4$	1

J^{Γ_7}	$(53)\Gamma_5$
$(53)\Gamma_5$	-1

J^{Γ_7}	$(55)\Gamma_3$
$(55)\Gamma_3$	1

J^{Γ_7}	$(13)\Gamma_3$	$(33)\Gamma_3$
$(13)\Gamma_3$	0	-1
$(33)\Gamma_3$		0

J^{Γ_7}	$(55)\Gamma_4$	$(55)\Gamma_5$
$(55)\Gamma_4$	$-\frac{1}{2}$	$-\sqrt{3}/2$
$(55)\Gamma_5$		$\frac{1}{2}$

J^{Γ_7}	$(15)\Gamma_5$	$(35)\Gamma_5$	$(35)\Gamma_4$
$(15)\Gamma_5$	0	$-1/\sqrt{2}$	$1/\sqrt{2}$
$(35)\Gamma_5$		$-\frac{1}{2}$	$-\frac{1}{2}$
$(35)\Gamma_5$			$-\frac{1}{2}$

J^{Γ_8}	$(11)\Gamma_1$	$(31)\Gamma_3$
$(11)\Gamma_1$	0	1
$(31)\Gamma_3$		0

J^{Γ_8}	$(55)\Gamma_1$	$(55)\Gamma_3$
$(55)\Gamma_1$	0	1
$(55)\Gamma_3$		0

J^{Γ_8}	$(51)\Gamma_5$	$[(51)\Gamma_5]'$
$(51)\Gamma_5$	$\frac{4}{5}$	$-\frac{3}{5}$
$[(51)\Gamma_5]'$		$-\frac{4}{5}$

J^{Γ_8}	$(53)\Gamma_5$	$[(53)\Gamma_5]'$
$(53)\Gamma_5$	$\frac{4}{5}$	$-\frac{3}{5}$
$[(53)\Gamma_5]'$		$-\frac{4}{5}$

J^{Γ_8}	$(53)\Gamma_4$	$[(53)\Gamma_4]'$
$(53)\Gamma_4$	$\frac{4}{5}$	$-\frac{3}{5}$
$[(53)\Gamma_4]'$		$-\frac{4}{5}$

J^{Γ_8}	$(13)\Gamma_3$	$(33)\Gamma_1$	$(33)\Gamma_3$
$(13)\Gamma_3$	0	$1/\sqrt{2}$	0
$(33)\Gamma_1$		0	$-1/\sqrt{2}$
$(33)\Gamma_3$			

J^{Γ_8}	$(15)\Gamma_5$	$[(15)\Gamma_5]'$	$(35)\Gamma_5$	$[(35)\Gamma_5]'$	$(35)\Gamma_4$	$[(35)\Gamma_4]'$
$(15)\Gamma_5$	0	0	$4/5\sqrt{2}$	$-3/5\sqrt{2}$	0	$1/\sqrt{2}$
$[(15)\Gamma_5]'$		0	$-3/5\sqrt{2}$	$-4/5\sqrt{2}$	$-1/\sqrt{2}$	0
$(35)\Gamma_5$			$\frac{2}{5}$	$-\frac{3}{10}$	0	$-\frac{1}{2}$
$[(35)\Gamma_5]'$				$-\frac{2}{5}$	$\frac{1}{2}$	0
$(35)\Gamma_4$					$-\frac{2}{5}$	$\frac{3}{10}$
$[(35)\Gamma_4]'$						$\frac{2}{5}$

J^{Γ_8}	$(55)\Gamma_5$	$[(55)\Gamma_5]'$	$(55)\Gamma_4$	$[(55)\Gamma_4]'$
$(55)\Gamma_5$	$-\frac{2}{5}$	$\frac{3}{10}$	$\sqrt{3}/2$	0
$[(55)\Gamma_5]'$		$\frac{2}{5}$	0	$-\sqrt{3}/2$
$(55)\Gamma_4$			$\frac{2}{5}$	$\frac{3}{10}$
$[(55)\Gamma_4]'$				$-\frac{2}{5}$

[a]For $\Gamma_e=\Gamma_4$ or Γ_5, the product $\Gamma_e\times\Gamma_8$ includes two Γ_8 representations; the two corresponding product states for arbitrary electron configurations $[(ij)\Gamma_e,\Gamma_8]\Gamma_8$ and $[(ij)\Gamma_e,\Gamma_8]\Gamma'$ are denoted by $(ij)\Gamma_e$ and $[(ij)\Gamma_e]'$, respectively.

TABLE VII. Coupling matrices of the electron-hole interaction $v(1,3)$ calculated for Ge; all notations are the same as in Table VI. The J^{Γ_7} matrices are omitted, because they are the same as the J^{Γ_6} matrices.

J^{Γ_6}	$(51)\Gamma_5$
$(51)\Gamma_5$	1

J^{Γ_6}	$(15)\Gamma_5$	$(55)\Gamma_5$	$(55)\Gamma_3$	$(55)\Gamma_4$
$(15)\Gamma_5$	0	$1/\sqrt{2}$	$1/\sqrt{3}$	$1/\sqrt{6}$
$(55)\Gamma_5$		$\frac{1}{2}$	$-1/\sqrt{6}$	$-1/2\sqrt{3}$
$(55)\Gamma_3$			0	$1/\sqrt{2}$
$(55)\Gamma_4$				$-\frac{1}{2}$

J^{Γ_8}	$(11)\Gamma_1$	$(51)\Gamma_5$	$[(51)\Gamma_5]'$
$(11)\Gamma_1$	0	$-1/\sqrt{5}$	$2/\sqrt{5}$
$(51)\Gamma_5$		$-\frac{4}{5}$	$-\frac{2}{5}$
$[(51)\Gamma_5]'$			$-\frac{1}{5}$

J^{Γ_8}	$(55)\Gamma_1$	$(55)\Gamma_3$	$(55)\Gamma_4$	$[(55)\Gamma_4]'$	$(55)\Gamma_5$	$[(55)\Gamma_5]'$	$(15)\Gamma_5$	$[(15)\Gamma_5]'$
$(55)\Gamma_1$	0	0	0	0	$-\sqrt{2}/15$	$2\sqrt{2}/\sqrt{15}$	$-1/\sqrt{15}$	$2/\sqrt{15}$
$(55)\Gamma_3$		0	$\sqrt{2}/\sqrt{5}$	$1/\sqrt{10}$	$-\sqrt{2}/\sqrt{15}$	$-1/\sqrt{30}$	$2/\sqrt{15}$	$1/\sqrt{15}$
$(55)\Gamma_4$			$\frac{2}{5}$	$\frac{1}{5}$	$\sqrt{3/5}$	$-1/5\sqrt{3}$	$-\sqrt{6/5}$	$\sqrt{2}/5\sqrt{3}$
$[(55)\Gamma_4]'$				$\frac{1}{10}$	$-1/5\sqrt{3}$	$3\sqrt{3}/10$	$\sqrt{2}/5\sqrt{3}$	$-3\sqrt{6}/10$
$(55)\Gamma_5$					$-\frac{2}{5}$	$-\frac{1}{5}$	$-2\sqrt{2}/5$	$-\sqrt{2}/5$
$[(55)\Gamma_5]'$						$-\frac{1}{10}$	$-\sqrt{2}/5$	$-\sqrt{2}/10$
$(15)\Gamma_5$							0	0
$[(15)\Gamma_5]'$								0

Let us now consider the electron-hole interaction with the electron (labeled 1) being in a valley (labeled by i), with an envelope wave function denoted by $\beta^i_m(\vec{r}_1)$, where the major axis of the ellipsoidal charge distribution is taken to be $\hat{z}_i$. If we choose the quantization axis of the hole $\hat{z}_3$ to be parallel to $\hat{z}_i$, then the potential seen by the hole, defined by

$$V_h^{m'm}(\vec{r}_3)\equiv\int \beta^{i*}_{m'}(\vec{r}_1)\beta^i_m(\vec{r}_1)v(1,3)d^3r_1 \tag{A2}$$

will not mix its four partners (labeled by $\pm\frac{1}{2}$ and $\pm\frac{3}{2}$) of the Γ_8 representation. Namely, we can write

$$\langle\beta^i_{m'}\phi^{\mu'_h}_{p'}\,|\,v(1,3)\,|\,\beta^i_m\phi^{\mu_h}_p\rangle=V_{13}(m'p',mp)\delta_{\mu_h,\mu'_h}(-1)^{|\mu_h|+1/2}\,, \tag{A3}$$

where

$$V_{13}(m'p',mp)=\begin{cases}\int f^*_{p'}(r_3)V_h^{m'm}(\vec{r}_3)f_p(r_3)\dfrac{d^3r_3}{(4\pi)} & \text{when } l'=l\\ \int f^*_{p'}(r_3)V_h^{m'm}(\vec{r}_3)f_p(r_3)Y^*_{00}(\Omega_3)Y_{20}(\Omega_3)d^3r_3/\sqrt{5} & \text{when } l'\neq l\,,\end{cases} \tag{A4}$$

with l' and l (restricted to 0 or 2) being the angular momenta associated with p' and p, respectively. Since the electron basis functions $\beta^{\mu_1}_m(\vec{r}_1)$ [defined in Eq. (17)] are linear combinations of the envelope functions $\beta^i_m(\vec{r}_1)$ localized at different valleys and oriented along different axes $\hat{z}_i$, the electron-hole interaction can be written in general as

$$\langle\beta^{\mu'_1}_{m'}\phi^{\mu'_h}_{p'}\,|\,v(1,3)\,|\,\beta^{\mu_1}_m\phi^{\mu_h}_p\rangle=j(\mu_1,\mu'_1;\mu_h,\mu'_h)V_{13}(m'p',mp)\,, \tag{A5}$$

where the coupling coefficients $j(\mu_1,\mu_1';\mu_h,\mu_h')$ can be determined by symmetry. To obtain these j coefficients, we need to know the transformation properties of the matrix elements under the operations in T_d. For simplicity, we drop out the indices $(m'p,mp)$ in Eq. (A5) and denote $V_{13}(m'p',mp)$ as V_{ss}, V_{dd}, and V_{sd}, respectively, for the cases $(l'=l=0)$, $(l'=l=2)$, and $(l'\neq l)$. If we transform the coordinate frame of the hole by a rotation about the y axis of an angle β, and then followed by a rotation about the new z axis of an angle γ, the potential $V_h(\vec{r}_3)$ will mix the four partners of the hole state in the following way:

$$
\begin{aligned}
&\langle \phi_\sigma^{'\mu_h'} \mid V_h(\vec{r}_3) \mid \phi_\sigma^{\mu_h} = V_{\sigma\sigma}\delta_{\mu_h\mu_h'}, \text{ for } \sigma=s,d \ , \\
&\langle \phi_s'^{\pm 1/2} \mid V_h(\vec{r}_3) \mid \phi_d^{\pm 3/2}\rangle = -\sqrt{2}d^{(2)}_{0\pm 1}(\beta)V_{sd}e^{\pm i\gamma} \ , \\
&\langle \phi_s'^{\pm 3/2} \mid V_h(\vec{r}_3) \mid \phi_d^{\pm 1/2}\rangle = \sqrt{2}d^{(2)}_{0\pm 1}(\beta)V_{sd}e^{\mp i\gamma} \ , \\
&\langle \phi_s'^{\pm 1/2} \mid V_h(\vec{r}_3) \mid \phi_d^{\mp 3/2}\rangle = \sqrt{2}d^{(2)}_{0\mp 2}(\beta)V_{sd}e^{\mp 2i\gamma} \ , \\
&\langle \phi_s'^{\mp 3/2} \mid V_h(\vec{r}_3) \mid \phi_d^{\pm 1/2}\rangle = \sqrt{2}d^{(2)}_{0\pm 2}(\beta)V_{sd}e^{\pm 2i\gamma} \ ,
\end{aligned}
\tag{A6}
$$

where the d matrices are defined in Ref. 37. Substituting Eqs. (17), (A2), and (A6) into Eq. (A5), we readily obtain the j coefficients. For the s-s and d-d terms, we obtain no couplings, i.e.,

$$
j(\mu_1,\mu_1';\mu_h,\mu_h') = \delta_{\mu_1\mu_1'}\delta_{\mu_h\mu_h'} \ .
$$

The coupling occurs for the s-d term, and these coefficients $j(\mu_1,\mu_1';\mu_h,\mu_h')$ can be found in Ref. 38.

The basis states for the D^0X are linear combinations of the products of two-electron states and hole states, which transform according to irreducible representation of T_d, i.e.,

$$
\mid mnp;[(\tau_1\tau_2)\Gamma_e^{\pm}\Gamma_h]\Gamma^{\pm}\mu\rangle = \sum_{\mu_e\mu_h} C_{\Gamma_e\Gamma_h}(\mu_e\mu_h,\Gamma\mu) \mid mn;(\tau_1\tau_2)\Gamma_e^{\pm}\mu_e\rangle \mid p;\Gamma_h\mu_h\rangle \ , \tag{A7}
$$

where $\mid mn;(\tau_1\tau_2)\Gamma_e\mu_e\rangle$ is the two-electron product states defined in the text and $\mid p;\Gamma_h\mu_h\rangle$ is the hole state given by (A1). Therefore, the matrix elements for electron-hole interaction are

$$
\begin{aligned}
&\langle m'n'p';[(\tau_1'\tau_2')\Gamma_e'^{\pm}\Gamma_h']\Gamma^{\pm}\mu \mid v(1,3) \mid mnp;[(\tau_1\tau_2)\Gamma_e^{\pm}\Gamma_h]\Gamma^{\pm}\mu\rangle \\
&\qquad = \sum_{\mu_e\mu_h} C_{\Gamma_e\Gamma_h}(\mu_e\mu_h,\Gamma\mu) \sum_{\mu_1\mu_2} C_{\tau_1\tau_2}(\mu_1\mu_2,\Gamma_e\mu_e) \sum_{\mu_e'\mu_h'} C_{\Gamma_e'\Gamma_h'}(\mu_e'\mu_h',\Gamma\mu) \\
&\qquad\quad \times \sum_{\mu_1'\mu_2'} C_{\tau_1'\tau_2'}(\mu_1'\mu_2',\Gamma_e'\Gamma_h') \\
&\qquad\quad \times \delta_{\tau_2\tau_2'}\delta_{\mu_2\mu_2'}\delta_{n'n} j(\mu_1,\mu_1';\mu_h,\mu_h') V_{13}(m'p',mp) f_{mn}^{\tau_1\tau_2} f_{m'n'}^{\tau_1'\tau_2'} \pm \cdots \ ,
\end{aligned}
\tag{A8}
$$

where the ellipsis represents an exchange term, $f_{mn}^{\tau_1\tau_2}$ is given by Eq. (12), and all the C coefficients can be found in Ref. 9. The exchange term is obtained from the first term by exchanging the roles of the two electrons in the final state. If we define an electron-hole coupling matrix for each overall symmetry Γ by

$$
\begin{aligned}
J^{\Gamma}([(\tau_1'\tau_2')\Gamma_e'\Gamma_h'],[(\tau_1\tau_2)\Gamma_e\Gamma_h] \equiv & \sum_{\mu_e\mu_h} C_{\Gamma_e\Gamma_h}(\mu_e\mu_h,\Gamma\mu) \sum_{\mu_1\mu_2} C_{\tau_1\tau_2}(\mu_1\mu_2,\Gamma_e\Gamma_e) \sum_{\mu_e'\mu_h'} C_{\Gamma_e'\Gamma_h'}(\mu_e'\mu_h',\Gamma\mu) \\
& \times \sum_{\mu_1'} C_{\tau_1'\tau_2'}(\mu_1'\mu_2,\Gamma_e'\mu_e') j(\mu_1,\mu_1';\mu_h,\mu_h') \ ,
\end{aligned}
\tag{A9}
$$

then Eq. (A8) reduces to

$$\langle m'n'p';[(\tau_1'\tau_2')\Gamma_e^{\pm}\Gamma_h']\Gamma^{\pm}\mu \mid v(13)mnp;[(\tau_1\tau_2)\Gamma_e^{\pm}\Gamma_h]\Gamma^{\pm}\mu\rangle$$

$$=J^{\Gamma}([(\tau_1'\tau_2')\Gamma_e'\Gamma_h'],[(\tau_1\tau_2)\Gamma_e\Gamma_h])V_{13}(m'p',mp)\delta_{\tau_2\tau_2'}\delta_{mn'}f_{mn}^{\tau_1\tau_2}f_{m'n'}^{\tau_1'\tau_2'}\pm\cdots,$$

where the ellipsis represents an exchange term. The electron-hole coupling matrices (J matrices) are listed in Tables VI for Si and VII for Ge, respectively.

---

*Present address: Department of Physcis, University of Illinois, Urbana, IL. 61801.

[1]J. R. Haynes, Phys. Rev. Lett. 4, 361 (1960).
[2]P. J. Dean, J. R. Haynes, and W. F. Flood, Phys. Rev. 161, 711 (1967).
[3]A. S. Kaminskii, Ya. E. Pokrovskii, and N. V. Alkeev, Zh. Eksp. Teor. Fiz. 59, 1937 (1970); [Sov. Phys.—JETP 32, 1048 (1971)].
[4]R. Sauer, Phys. Rev. Lett. 31, 376 (1973).
[5]K. Kosai and M. Gershenzon, Phys. Rev. B 9, 723 (1974).
[6]P. J. Dean, D. C. Herbert, D. Bimberg, and W. J. Choyke, Phys. Rev. Lett. 37, 1635 (1976).
[7]G. Kirczenow, Solid State Commun. 21, 713 (1977); Can. J. Phys. 55, 1787 (1977).
[8]M. L. W. Thewalt, in *Proceedings of the 14th International Conference of Physics Semiconductors, Edinburgh, 1978,* edited by B. L. H. Wilson (Institute of Physics and Physical Society, London, 1979), p. 605.
[9]Throughout this paper we will adopt the notations used by G. F. Koster, J. O. Dimmock, R. G. Wheeler, and H. Statz, *Properties of the Thirty-two Point Groups,* (Cambridge, Mass., 1963).
[10]A. E. Mayer and E. C. Lightowlers, J. Phys. C. 12, L539 (1979); 12, L946 (1979).
[11]Y. C. Chang and T. C. McGill, preceding paper, Phys. Rev. B 25, 3927 (1982).
[12]Y. C. Chang and T. C. McGill, Phys. Rev. Lett. 45, 471 (1980).
[13]See, for example, J. M. Ziman, *Principles of the Theory of Solids* (Cambridge University Press, London, 1972), Chap. 5.
[14]In the present calculation, we use the empirical form for $\epsilon(\vec{q})$ obtained by Vinsome and Richardson (Ref. 15).
[15]P. K. W. Vinsome and D. Richardson, J. Phys. C 4, 2650 (1971).
[16]S. T. Pantelides and C. T. Sah, Phys. Rev. B 10, 621 (1974); 10, 638 (1974).
[17]A. Baldereschi and N. O. Lipari, Phys. Rev. B 8, 2697 (1973); 9, 1525 (1974).
[18]J. M. Luttinger, Phys. Rev. 102, 1030 (1956).
[19]See, for example, P. M. Morse and H. Feshbach, *Methods of Theoretical Physics* (McGraw-Hill, New York, 1953), p. 928.
[20]Y. C. Chang, T. C. McGill, and D. L. Smith, Phys. Rev. B 23, 4169 (1981).
[21]N. O. Lipari and M. Altarelli, Phys. Rev. B 15, 4883 (1977).
[22]M. Altarelli and N. O. Lipari, Phys. Rev. B 15, 4898 (1977).
[23]E. C. Lightowlers, M. O. Henry, and M. A. Vouk, J. Phys. C 10, L713 (1977); 10, L945 (1979).
[24]M. L. W. Thewalt, Solid State Commun. 21, 937 (1977); Can. J. Phys. 55 1463 (1977).
[25]K. R. Elliott and T. C. McGill, Solid State Commun. 28, 491 (1978).
[26]R. L. Aggarwal, P. Fisher, V. Vourzine, and A. K. Randas, Phys. Rev. A 138, 882 (1965).
[27]M. L. W. Thewalt, Solid State Commun. 28, 361 (1978).
[28]S. A. Lyon, D. L. Smith, and T. C. McGill, Solid State Commun. 28, 317 (1978).
[29]M. O. Henry and E. C. Lightowlers, J. Phys. C 12, L485 (1979).
[30]R. L. Aggarwal and A. K. Ramdas, Phys. Rev. 140, A1246 (1965).
[31]K. L. Shaklee and B. Nahory, Phys. Rev. Lett. 24, 942 (1970).
[32]Y. C. Chang and T. C. McGill, Solid State Commun. 30, 187 (1979).
[33]R. A. Faulkner, Phys. Rev. 184, 713 (1969).
[34]A. E. Mayer and E. C. Lightowlers, J. Phys. C (in press).
[35]J. H. Reuszer and P. Fisher, Phys. Rev. 135, A1125 (1964).
[36]G. A. Thomas, A. Frova, T. C. Hensel, R. E. Miller, and P. A. Lee, Phys. Rev. B 13, 1962 (1976).
[37]A. R. Edmonds, *Angular Momentum in Quantum Mechanics* (Princeton University Press, Princeton, N.J., 1957), Chap. 4.
[38]Yia-Chung Chang, Doctoral thesis, California Institute of Technology, 1981 (unpublished).